RESEARCH REVIEW JOURNALS
Volume-04
Issue-04
April-2019

ISSN: 2455-3085 (Online)
RESEARCH REVIEW International Journal of Multidisciplinary
www.rrjournals.com [UGC Listed Journal]

Study of Undopped ZnO Thin Films

[1]KM Deepika Mishra and [2]Dr. Pawan Kumar Singh

[1]*Research Scholar, Department of Physics, Sri Satya Sai University of Technology & Medical Sciences, Sehore, M.P.*
[2]*Research Guide, Department of Physics, Sri Satya Sai University of Technology & Medical Sciences, Sehore, M.P.*

ARTICLE DETAILS

Article History
Published Online: 15 April 2019

Keywords
emission, transmission, diffraction.

ABSTRACT

A multifunctional material is Nanostructured zinc oxide (ZnO), can be produced as ferromagnetic, piezoelectric, transparent and performed by proper doping or alloy. Due to their wide range of practical applications in photonic crystals, the semiconductor ZnO has achieved considerable interest in the research. This paper reflects study of undopped ZNO thin films.

I. INTRODUCTION

ZnO lacks strong visible wavelength clarity, is a vital resource for diverse photonic applications. Not only does it find use in various associated photonic technologies, but it can also be used efficiently as a sensor in numerous MEMS-related devices due to its piezoelectric nature. The films nanostructured by ZnO show high quality crystalline. We display a strong excitonic UV emission at 383 nm (3.25 eV).

II APPLICATION OF EXPERIMENTAL TECHNIQUES FOR ZNO THIN FILMS PREPARATION

By preparing the starting sol of appropriate consistency, ZnO nanocrystalline thin films is synthesised. The precursor solution was prepared by combining 2.1949g dihydrate ($Zn(CH_3COO)_2$ with zinc acetate. $2H_2O$) and just a few drops of ethanol diethanolamine. The formulated solution was continuously stirred at 50°C for one hour and aged for one day before being used as the starting sol in spin-coating process. The glass substrates used for coating were first coated in a combined solution of HCl and HNO_3 and regularly washed many times in purified water and ethanol. The glass substrates were dried even farther and a thin, uniform ZnO film was stored by a rotated spin coater with a highest speed of 3000 rpm for 30s. Sample preparation with the first annealing process is clarified as follows. Each coating of ZnO film was spin-coated on the substratum, preceded by a 1min drying in air at 200°C and cooling back to room temperature. Above that the mentioned process of spinning and drying was proceeded 8 more times consecutively. Ultimately, all of the samples prepared were post-annealed in the ambient atmosphere for an hour at 350,450 and 5500C and allowed to cool down.

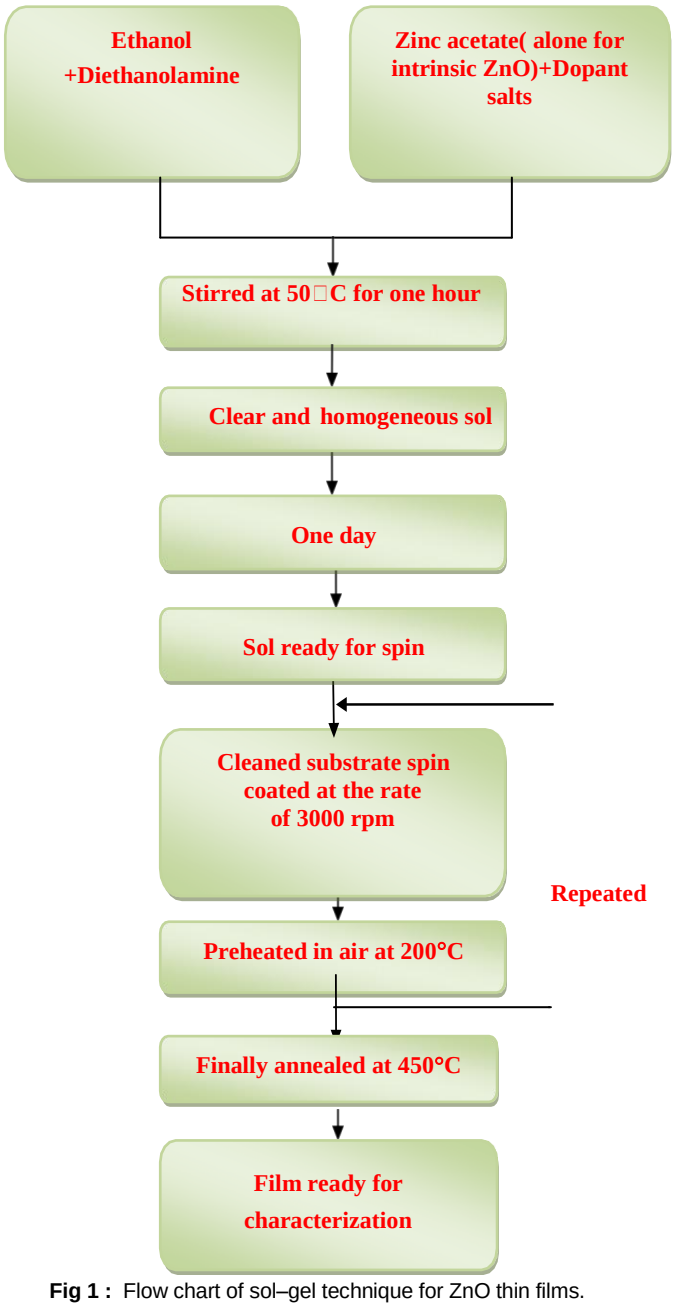

Fig 1 : Flow chart of sol–gel technique for ZnO thin films.

RRIJM 2015, All Rights Reserved

III CHARACTERIZATIONS

The sample crystal structure was analyzed via x-ray diffractometer (XRD- XPERT-PRO) in the 20-80° angle (2) range via wavelength 0.15405 nm CuKα radiation. For morphological findings of the ZnO, field emission scanning electron microscope (FESEM) and a transmission electron microscope (TEM- JEOL 2010) were used. Utilising FESEM-JEOL- 6460F the SEM images of the sol – gel dependent films were obtained. Energy dispersive spectroscopy (EDX) was also performed in the same room. In the wavelength range of 350-850 nm, the optical transmission spectra of ZnO films is recorded by using UV-VIS spectrophotometer (JASCO V 570). The photoluminescence spectra was used to research the luminescent activity of the films using the photoluminescence spectrometer (Varian Cary Eclipse- EL08083851) where a Xenon lamp is being used as the source of light as well as the films were excited with a wavelength of 280 nm. All of the spectra were collected by holding the samples in the atmosphere surrounding them. A vibrating sample magnetometer (VSM-Lakeshore-7404) was used to perform magnetisation tests.

IV RESULTS

1. STRUCTURAL PROPERTIES OF THE CRYSTALLINE ZNO THIN FILM

Utilizing patterns of X-ray diffraction (XRD), the crystal structure and orientation of the ZnO thin film as prepared and annealed samples at 350, 450 and 550°C were explored. Figure 2 displays the patterns of X-ray diffraction for the crystalline ZnO thin films, and shows that the films are polycrystalline in nature and have a single layer hexagonal hexagonal wartzite framework. From the figure it is clear that the crystallinity of ZnO films tends to increase with the rise in the temperature of the annealing.

For the as-deposited film three peaks appear on the pattern of XRD. As seen in Figure 2(a), the ZnO thin film as able to prepare has (101) as its preferred orientation, whereas the other orientations like (100) and (002) are also viewed relatively with lower intensities. Besides that, almost all of the thin ZnO films that develop with wartzite structure have a preferential orientation (002). The temperature of the annealing plays a critical role in surface reactions and the mobility of species. Figure 2 (b & c) indicates that the ZnO films have (002) planes as the favoured orientation and other extreme peaks correspond to the (100) and (101) plane orientations.

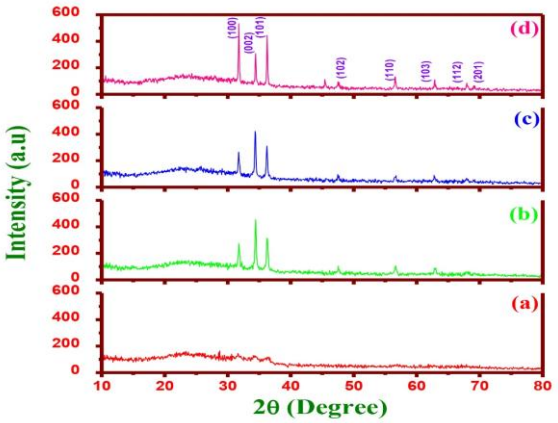

Fig 2 : (a-d) XRD patterns of ZnO thin films. (a) as- prepared, annealed (b)at 350°C (c)at 450°C (d)at 550°C

Then there are also several peaks of low strength relating to the orientations (102), (110) and (103). It is found that the prominent point of (100) orientation plane and peaks of other orientations also occur in Fig 2d and refers to the XRD pattern of the ZnO thin film annealed at 550°C. Thus, it can be said that annealing leads to increases in plane intensity and reorientation, and a similar observation is noted by others as well **[Yakuphanoglu et al., 2007].** The lattice constants 'a' and 'c' for spin-coated ZnO thin films were calculated using an analytical method **[Ilican et al. 2007].** The values of 'a' and 'c' lattice constants for the films as prepared and annealed at various temperatures are determined using equation and the measured values are given in Table 1. Compared to the hexagonal ZnO crystal lattice constants given in the standard data file JCPDS (36-1451) a = 3.2498 Å and c= 5.2066Å, the measured values are in good accordance with the standard values for ZnO wurtzite structure.

Table 1: Lattice constant values of ZnO thin films.

Lattice Parameter	Standard value (Å)	As prepared (Å)	At 350°C (Å)	At 450°C (Å)	At 550°C (Å)
a	3.2498	3.2536	3.2508	3.2543	3.2525
c	5.2066	5.2233	5.2089	5.2111	5.2097

For all films the relative percentage error for the observed and JCPDS standard d – value [36-1451] is computed using the equation [5] and given in Table 2.

The size of crystallites is determined using Scherrer's well-known formula as given in equation. The size of grain varies between 9 and 72 nm. The size of grain results are calculated in Table 3 for all the films. Comparison to the annealed films, the grain size of the as-prepared ZnO thin film is extremely small. The size of the grain increases as the temperature of the annealing rises which is well supported in literature [Krunks et al., 2006]. The size of grain varied with annealing temperature of ZnO crystallites is given in Table.3.

The texture coefficient (TC) describes the texture of the particular plane, through which the desired development means a divergence from unity. Quantitative data on the preferential orientation of crystallite was obtained from the various texture coefficient TC(hkl) defined by the relationship and measured value are provided in table 4.

RRIJM 2015, All Rights Reserved

Table 2: Interplanar spacing of various planes for the ZnO thin films.

Samples	Without Annealing			Annealed at 350°C			Annealed at 450°C			Annealed at 550°C		
(hkl)	2□	d(Å)	d%	2□	d(Å)	d%	2□	d(Å)	d%	2□	d(Å)	d%
(100)	31.7575	2.81772	0.12	31.7588	2.81528	0.03	31.7259	2.81813	0.14	31.7416	2.81677	0.08
(002)	34.3086	2.61166	0.3	34.4060	2.60449	0.04	34.3510	2.60854	0.20	34.4008	2.60487	0.06
(101)	36.2506	2.47608	0.4	36.2406	2.47674	0.4	36.1936	2.47985	0.57	36.2376	2.47694	0.4

Table 3: FWHM, d-spacing and Particle size (D) for pure ZnO

(hkl)	As Prepared ZnO		Annealed at 350□C		Annealed at 450□C		Annealed at 550□C	
	β(FWHM)	D (nm)	β(FWHM)	D (nm)	β(FWHM)	D (nm)	β(FWHM)	D (nm)
(100)	0.5904	14	0.2904	29	0.2023	41	0.1258	66
(002)	0.9885	8	0.2147	39	0.1757	47	0.1149	72
(101)	0.9297	9	0.2509	33	0.1837	46	0.1173	71

Table 4: Texture coefficient of ZnO thin films

(hkl)	ZnO Thin film annealed at							
	Without Annealing		350□C		450□C		550□C	
	(I/I_o)	TC_{hkl}	(I/I_o)	TC_{hkl}	(I/I_o)	TC_{hkl}	(I/I_o)	TC_{hkl}
(100)	77.25	0.8447	45.55	0.6345	47.91	0.6635	100	1.2398
(002)	97.12	1.0619	100	1.3931	100	1.3848	55.13	0.6835
(101)	100	1.0934	69.80	0.9724	68.72	0.9517	86.84	1.0766

Figure 3 shows the as-prepared FESEM micrographs and the calcined ZnO nanocrystalline thin films at 350, 450, 550°C for 1h, respectively. It is observed that film annealed at 450°C displays strong homogeneity of hexagonally formed grains well scattered on the film's surface. Compares favorably with other videos, the sample morphology annealed at 450°C is stronger. Hence, for the further study, all the samples are annealed at 450ºC.

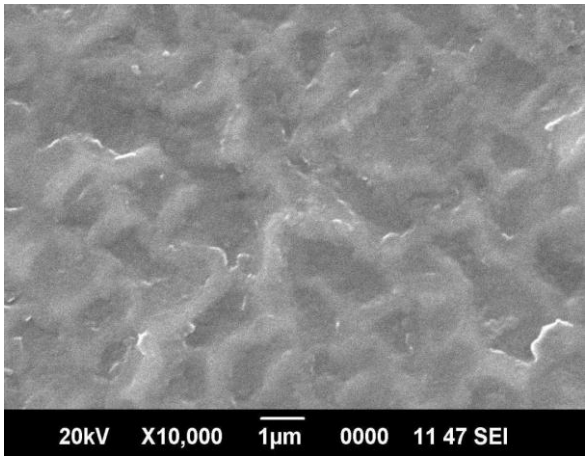

Fig 3 (a) SEM micrograph of ZnO thin film of as prepared

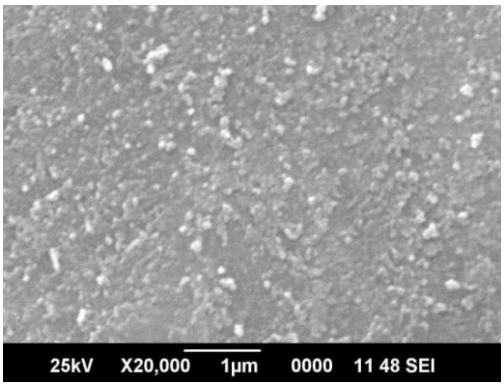

Fig 3 (b) SEM micrograph of ZnO thin film calcined at 350°C

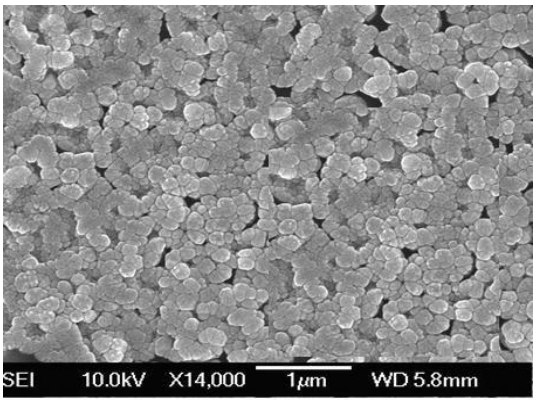

Fig 3 (c) SEM micrograph of ZnO thin film calcined at 450°C

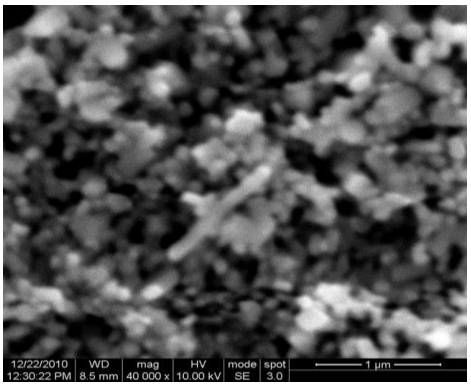

Fig 3 (d) SEM micrograph of ZnO thin film calcined at 550°C

2 OPTICAL PROPERTIES

Figure 4 shows the transmittance spectra of ZnO thin films, taken in the range of wavelengths from 350 to 850 nm. In the visible range of the electromagnetic spectrum, the films are extremely translucent with an overall propagation value of up to 80 per cent. The ZnO film at 450 ° C shows a high transmittance while the image is hazy and the transmission for the ZnO film film annealed at 550°C **[Mingsong Wang *et al*., 2008].**

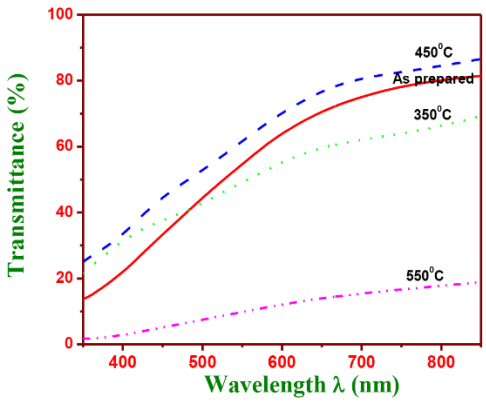

Fig 4 Transmittance spectra of ZnO thin film annealed at various temperature

Transmittance measurements have calculated the absorption coefficient α of ZnO films. Because the envelope technique is not valid in the high adsorption region, the measurement of the film's absorption coefficient α was computed by using expression in this region. Film thickness was calculated and the results micrometer (Mitutoyo, Japan). The film thicknesses were around 962,844,811 and 934 nm for the as prepared and annealed at 350,450 and 550°C, respectively. The values obtained of absorption coefficients are used to evaluate the gap of the prepared ZnO thin films in the optical energy band. Figure 4.5 (a-d) shows the plot of α^2 versus $h\nu$, where α as the optical absorption coefficient and h as the inc energy of the incident photon. The energy band-gap (E_g) was calculated by the expression, suggesting a direct transition between both the valence and conduction bands. For as packed, the deduced optical energy band-gap, Eg 2.75, 3.00, 3.13 and 2.50 eV, annealed at 350,450 and 550° C film respectively. Such values are significantly lower than the 3.37 eV bulk alue **[Krasimira Shtereva et al., 2009]** and match well with previously released ZnO thin film results.

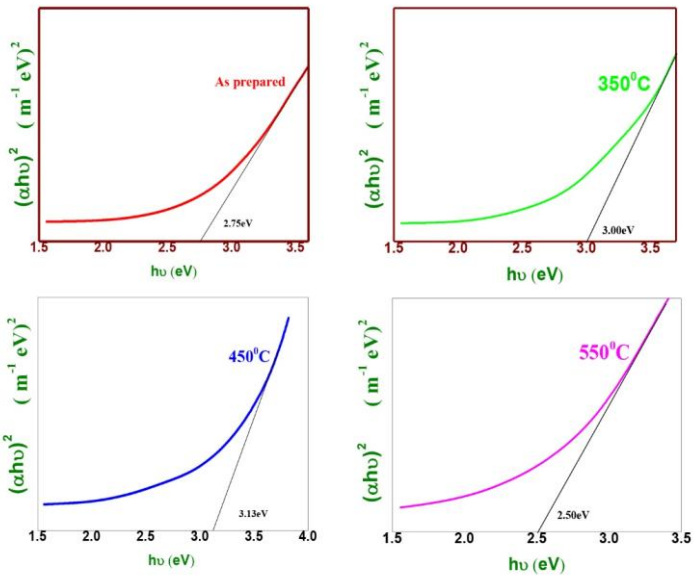

Fig. 5 Plots of absorption against photon energy for ZnO thin films

3. PHOTOLUMINESCENCE STUDIES OF ZNO THIN FILMS

Photoluminescence measurements were used to calculated the optical and crystalline quality of the ZnO layers deposited at different annealing temperatures. The excitation spectra shown in Fig 6 were obtained for the maximum emission wavelength indicated in Fig 7. All spectra show a peak around 383 nm (3.24 eV) resulting due to electron transfer from valence band (V_B) to conduction band (C_B) that could be the origin of any emission.

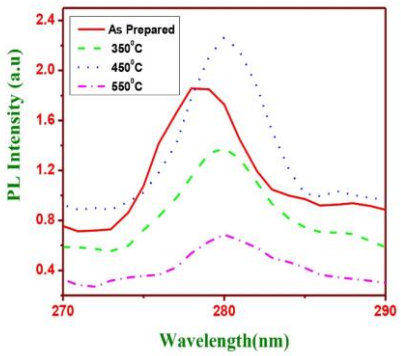

Fig 6 Photoluminescence excitation spectra for pure ZnO

There are two emission peaks for the as prepared film namely the defect peak which is of lower intensity compared with the strong near band edge (NBE) emission peak. The defect peak of as-prepared film has disappeared with the rise in annealing temperature, indicating the better quality of crystalline of the samples deposited at higher temperatures. PL intensity rises as the annealing temperature rises till 450°C. PL intensity decreases for the ZnO thin film annealed at 550°C as the film became hazy which is true for the transmission spectra also.

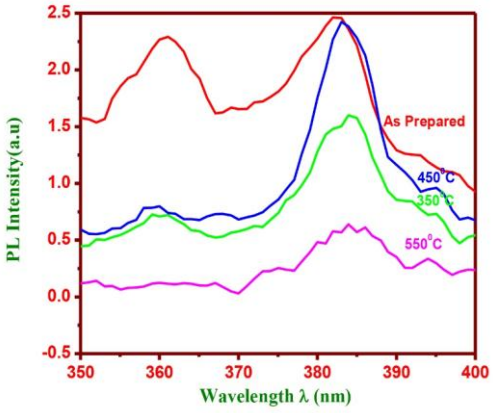

Fig 7 Room temperature photoluminescence emission spectra

Changes in relative intensities of the dominant peaks are observed. The peakm intensity at 383 nm decreases with the annealing temperature. Strong near band edge (NBE) emission dominates for all samples in the PL spectra taken at room temperature. Though the emission energy of the PL spectra does not change with rising annealing temperature (Fig. 4.7), the PL intensity varies with annealing temperature.

V PHYSICAL PROPERTIES OF ZNO HAVING DIFFERENT NUMBER OF LAYERS

1 STRUCTURAL PROPERTIES

XRD was characterized by the thin films ZnO to confirm the crystalline phase of the films. Figure 8 (a-e) indicates the representative XRD pattern of ZnO thin films synthesized at 450 über C, a film that reveals ZnO's phase of wartzite. The sharp summits of the XRD imply good crystallinity. The deposited ZnO films showed a crystalline nature, although with an increasing number of layers, the crystalline nature of the deposited ZnO films became more established and increasingly more extreme and clear for films with a maximum of up to eight layered depositions. Peaks were well defined and sharp for the ten layered film but slight decrease in intensity was observed. X-ray diffraction (XRD) has revealed a strong thickness effect on the topography of film surfaces. Structural analysis based on X-ray diffraction reveals that ZnO films have developed primarily in the course of the c-axis (002) where the angular orientation of the apex (002) differs marginally **[Mukes Kapilashrami *et al*., 2010].** As the film's thickness enhanced, the film's crystalline nature enhanced, which is also in keeping with the literature [Linhua Xu et al., 2011]. Table 5 gives the values of the lattice constants 'a' and 'c' for various layers determined using equation and the estimated values. Compared to the hexagonal ZnO crystal lattice constants given in the standard JCPDS data file a = 3.2498 Å and c= 5.2066 Å, it is apparent that the values obtained are in good agreement with the standard values for ZnO wartzite structure.

Table.5: Lattice constants of ZnO thin films.

Lattice constant	2 layers	4 layers	6 layers	8 layers	10 layers
a (Å)	3.24197	3.25955	3.25981	3.25430	3.24716
c (Å)	5.20150	5.21898	5.21990	5.21110	5.20734

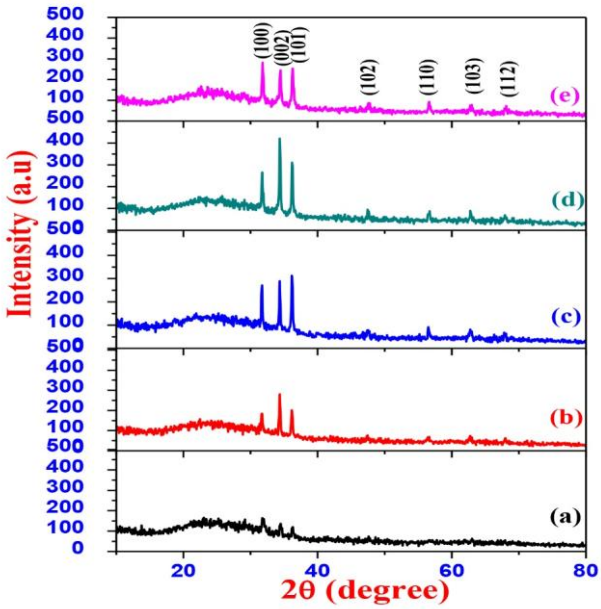

Fig 8 (a-e) XRD spectra of ZnO thin film of 2,4,6,8 and 10 layers annealed at 450□C.

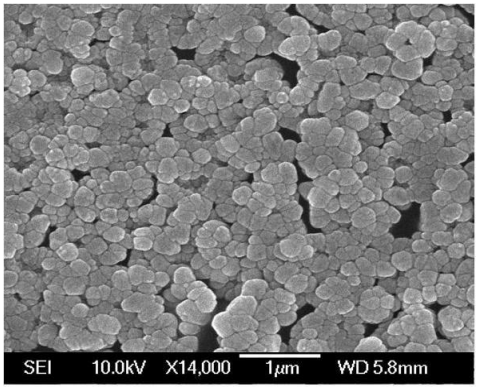

Fig 9(a) FESEM image of ZnO with 2 layers

The specific plane and details about the preferred orientation of crystallite were calculated by using equation from the texture coefficient TC(hkl) in Table 6. The size of particle (D) of the films with several layers was calculated by the Debye–Scherrer formula with the use of raw data from XRD patterns. The scrystalline size was calculated by the Debye–Scherrer formula along the dominant peaks (100), (002) and (101) is provided in Table 7.

FESEM has observed the surface morphology and micrographs of the ZnO thin films grown on glass substratum with various layers. Illustration. 9 (a-e) demonstrates the high morphology of 2,4,6,8, and 10-layer films. In all the thin film samples, the surface morphologies are distinct. The thin film's surface morphology developed up to 8 layers was more densely packed with some pits on it, whereas the one grown with 10 layers of slight agglomeration emerged [Mondal et al., 2008].

Table 6: Texture coefficient of ZnO thin films.

(hkl)	ZnO Thin film of various thickness									
	2 LAYER		4 LAYER		6 LAYER		8 LAYER		10 LAYER	
	(I/I_o)	TC_{hkl}	(I/I_o)	TC_{hkl}	(I/I_o)	TC_{hkl}	(I/I_o)	TC_{hkl}	(I/I_o)	TC_{hkl}
(100)	100.00	1.0782	47.80	0.6602	71.20	0.8486	47.91	.0.6635	97.88	1.0535
(002)	90.51	0.9758	100.00	1.3811	80.52	0.9596	100.00	1.3848	80.85	0.8702
(101)	87.74	0.9460	69.42	0.9588	100.00	1.1918	68.72	0.9517	100.00	1.0763

Table 7: 2□, FWHM, d-spacing and Particle size(D) of ZnO thin film

(hkl)	2 Layer			4 Layer			6 Layer			8 Layer			10 Layer		
	2□	β(FWHM)	D(nm)	2□	β(FWHM)	D(nm)	2□	β(FWHM)	D(nm)	2□	β(FWHM)	D(nm)	2□	β(FWHM)	D (nm)
(100)	31.8476	0.5053	16	31.6714	0.2317	36	31.6688	0.1606	51	31.7259	0.2023	41	31.7954	0.2262	37
(002)	34.4571	0.2479	34	34.3380	0.1754	47	34.3318	0.1486	56	34.3510	0.1757	47	34.4171	0.2814	30

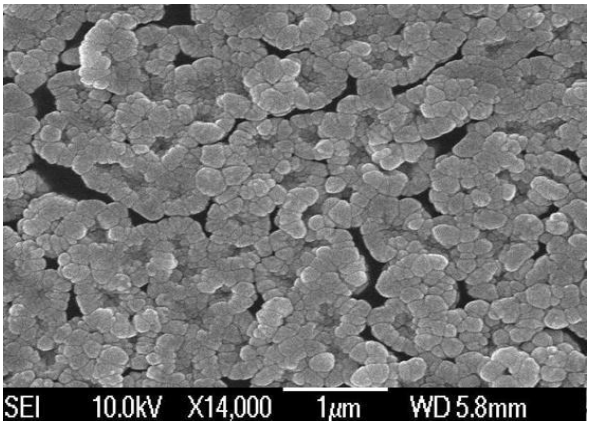

Fig 9(b) FESEM image of ZnO with 4 layers.

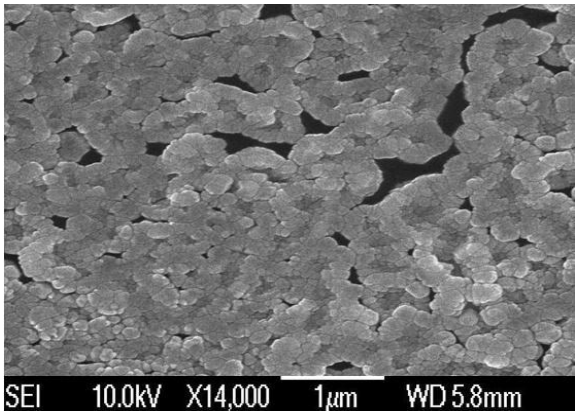

Fig 9(c) FESEM image of ZnO with 6 layers.

RRIJM 2015, All Rights Reserved

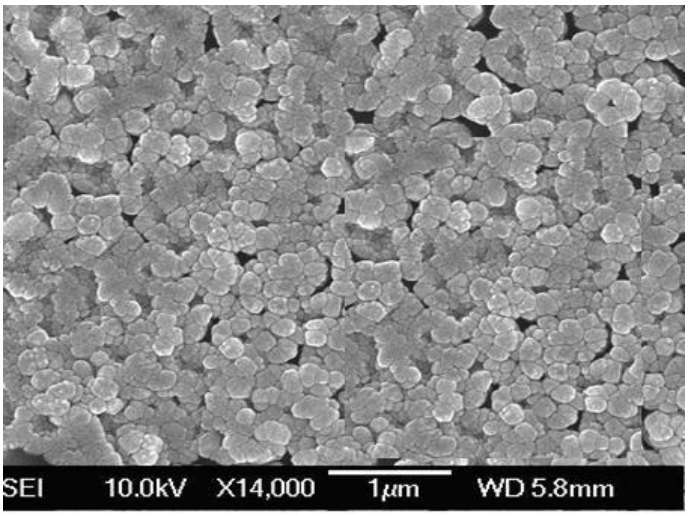

Fig 9(d) FESEM image of ZnO with 8 layers

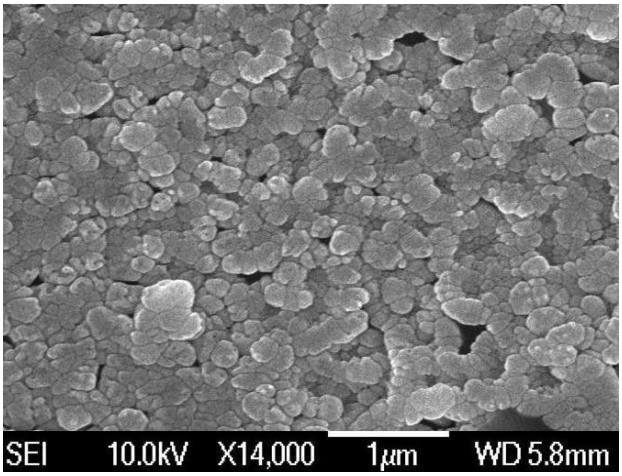

Fig 9(e) FESEM image of ZnO with 10 layers**.**

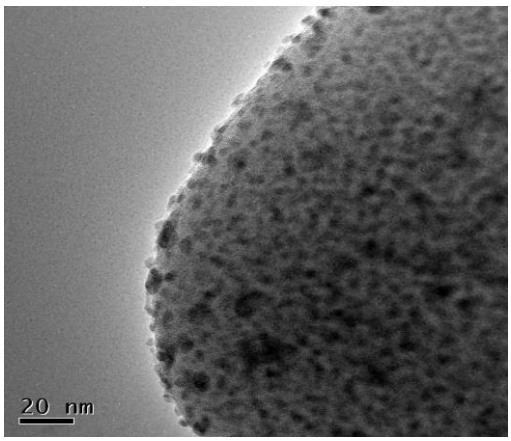

Fig 10 TEM image of ZnO thin film with 8 layers and calcined at 450°C

Transmission electron microscopy was employed to observe the microstructure of pure ZnO thin films with 8 layers annealed at 450ºC (Fig-10). ZnO powders obtained by scraping the coated film were dispersed in ethanol and some drops of the suspension were placed on carbon-coated copper grid which acted as the specimen holder for taking TEM image. The image was recorded with a JEOL-2010 microscope managed at 200 kV using a low-background Gatan double tilt holder. The TEM image confirms the nanocrystalline nature of pure ZnO films having particles of around 10 nm in dimension based on the scale given in the micrograph.

RRIJM 2015, All Rights Reserved

2 XPS ANALYSIS

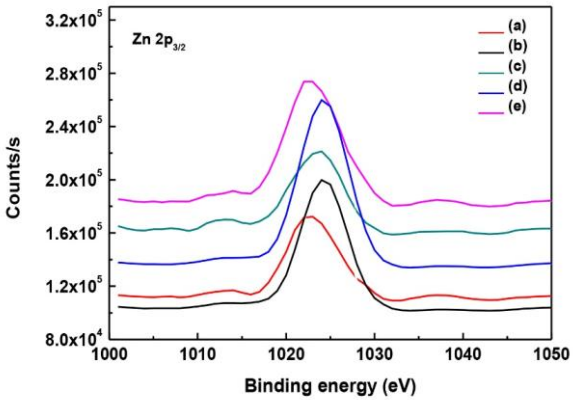

Fig 11 (a) XPS close scan spectra (Zn $2p_{3/2}$) of ZnO films with different thicknesses 2 layer, (b) 4 layer, (c) 6 layer (d) 8 layer, (e) 10 layer

To find the stoichiometry of ZnO films, quantitative analysis should be carried out using the XPS analysis of Zn $2p_{3/2}$ and O 1s energy lines respectively, it is shown in Fig 11(a) and Fig 11(b). In the current study, the observed Zn $2p_{3/2}$ peak located at 1022.58, 1024.16, 1023.61, 1024.16 and 1022.47 eV for the 2, 4, 6, 8 and 10 layers respectively, which is nearly the same as the standard value of 1021.8 eV. Also, O 1s peak positions are observed at 531.02, 529.96, 530.78, 531.05 and 531.12 eV for the 2, 4, 6, 8 and 10 layers respectivelyIt's really 'close the normal 530.05 eV rating. The amazing fact is that with the increasing thickness of the ZnO films, the XPS peak intensities rise. Observing these peaks of Zn $2p_{3/2}$ and O 1s indicate the formation of these elements in this studied ZnO film.The stoichiometry was found out from this peak, which gives the presence of Zn : O as 1.02 : 0.98.

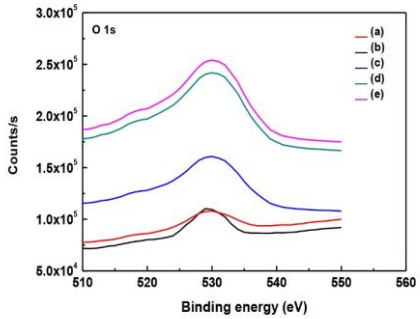

Fig 11(b) XPS close scan spectra (O 1s) of ZnO films with different thicknesses (a) 2 layer, (b) 4 layer, (c) 6 layer, (d) 8 layer and (e) 10 layer

.3 OPTICAL PROPERTIES

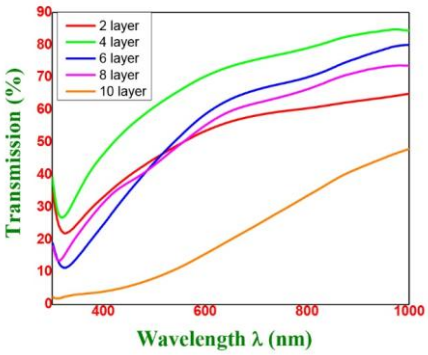

Fig 4.12 Optical transmission spectra of the ZnO multilayer thin films.

RRIJM 2015, All Rights Reserved

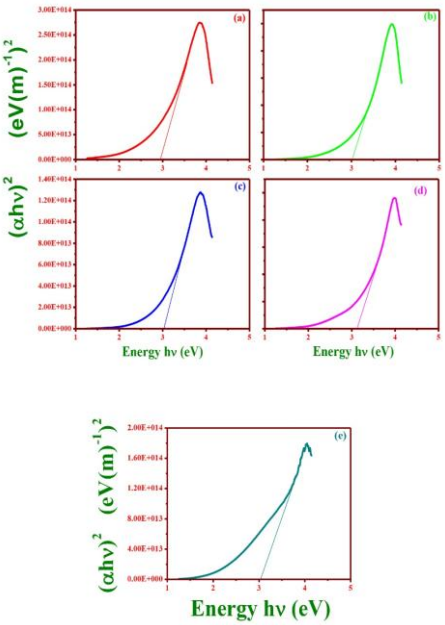

Fig 13 Variation of $(\alpha h\nu)^2$ of the ZnO (a) 2 layer (b) 4 layer (c) 6 layer (d) 8 layer (e)10 layer multilayer thin films as a function of photon energy (hν)

Figure 12 demonstrates the ZnO thin film optical transmission spectra utilizing UV-Vis - NIR spectrometer with different layers evaluated at room temperature. In the visible region, all the films show 60-80 percent transmission except for 10 layers. The band-gap energy (E_g) of the multilayer thin film was computed from the plot between □□ *h*□ □ ^{2} and *h*□, where α is the optical absorption coefficient and h corresponds to the energy of the incident photon. Assuming a simple transition among valence and conduction bands, the energy band difference (E_g) has been estimated from the expression, eg is calculated by extrapolating the straight line portion of the curve to $(\alpha h\square)^2 = 0$. Transmittance calculations have calculated the absorption coefficient α of ZnO films. While the envelope approach is not applicable in the heavy absorption region, the measurement of the film's absorption coefficient α was determined in this region by using expression. Figure 13 displays $(\alpha h\nu)^2$ ZnO thin film plots as a photon energy feature. The multilayer thin film energies achieved utilizing Fig 4.13 are 2.97, 3.03, 3.06, 3.13 and 3.03 eV for the ZnO thin films with 2,4,6,8 and 10 layers respectively. The band-gap energy obtained for pure ZnO in this research is lower than the ZnO value of 3.37 eV in bulk. In this research, as mentioned in the literature, the appropriate band-gap energy of multilayer thin films improved by increasing the number of layers of ZnO **[Bin-Zhong Dong *et al*., 2007].**

4 PHOTOLUMINESCENCE SPECTRA

In Fig 14 of the ZnO films, the PL spectra demonstrated UV emission peak for about 383 nm, luminescence green-yellow at 496 nm. The first increase due to UV emissions (near band edge-NBE) is related to band-to - band transitions, excitonic emissions and pair-transitions of donor-acceptors. The dark-yellow band at 496 nm is due to the dark region's deep-level emissions (DLE), which are related to oxygen vacancies, zinc vacancies or zinc interstitials **[Haiping Tang *et al*., 2008].** These two peaks are the most commonly found luminescent peaks in all the ZnO samples. In addition to these peaks one shoulder peak near the NBE, two shoulder peaks near DLE also appear. The excitonic emissions intensities and defects emissions decreases with increase the number of the layers and the shoulder peaks disappear for 8 & 10 layers. Since the ZnO layer is fairly small, the structural distortion is relatively wide and there are several interstitial Zn atoms that may result in the blue emission. The structural disorder decreases of film thickness, and the density of Zn interstitial defect is decreased. As a consequence the blue emission rate is also reduced.

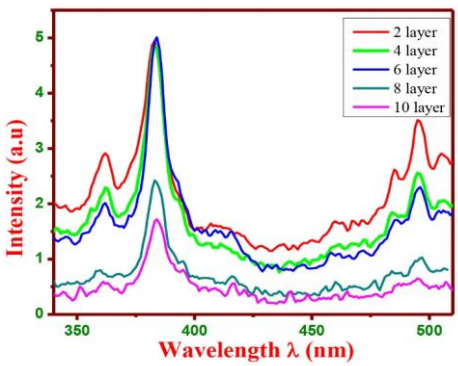

Fig 14 Room-temperature photoluminescence spectra of the samples.

5 MAGNETIC PROPERTIES

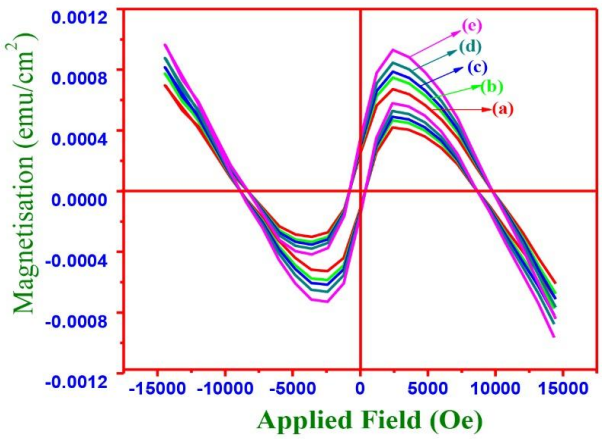

Fig15 Magnetic hysteresis loops of Pure ZnO thin films of various thicknesses at room temperature.

The samples prepared were handled carefully to avoid any possible magnetic contamination. The undoped ZnO films prepared were examined at room temperature (RT) in the span of the magnetic field 0–17.5 kOe with the use of a Vibrating Sample Magnetometer and showed non-ferromagnetic behavior, confirming that there is no extrinsic magnetic impurity contamination during the procedure of preparation presents the magnetization (M) vs magnetic field (H) of pure ZnO thin films with different thicknesses. Hysteresis curves are obtained at room temperature, showing all pure samples have non-ferromagnetic characteristic property. A typical diamagnetic behaviour has been identified in the bare ZnO samples. The diamagnetic behaviour of pure ZnO is due to the unpaired electrons of its d orbital, which is responsible for the absence of a permanent magnetic moment.

VI EFFECT OF DIFFERENT PROCESS OF ANNEALING

Additionally, the above annealing process, physical properties through hybrid annealing also studied. In the process of hybrid annealing, each layer of film was preheated with the use of a microwave oven by supplying a power of 900 W for 1min after each spin coating. The above process is repeated again for 8 more times after bringing down the substrate to room temperature. As a final step, all the samples were post- annealed in the microwave oven at a power of 900 W for 30 min and subsequently in open air at 450°C for 30 min which is termed as hybrid annealing. The annealed samples were brought to room temperature in a natural manner. The sample prepared in the normal and hybrid annealing processes were given the names A and B respectively.

1 STRUCTURAL PROPERTIES

X-ray diffraction patterns of the samples A and B are shown in Fig 16 Both the films show a diffraction peak at 31.86° which corresponds to the reflection of the (100) plane of the wurtzite structure of ZnO material.

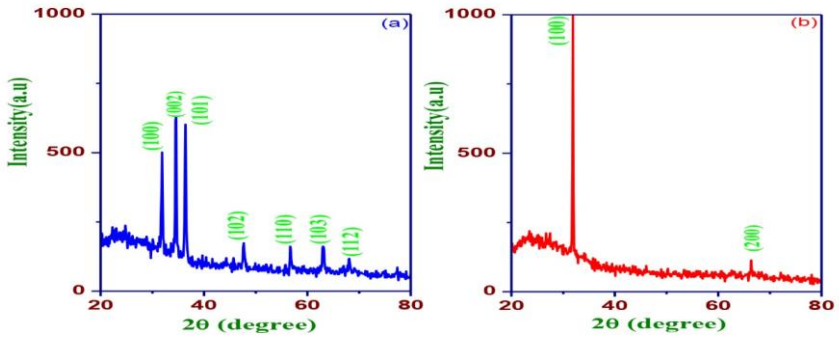

Fig 16 X-ray diffraction patterns of the samples A (a) and B(b)

Sample A shows polycrystalline behavior exhibiting wurtzite structure and all the observed XRD peaks are identified with their corresponding planes in the recorded range. This film indicated a greater orientation towards the (002) plane along the c-axis and other planes such as (100), (101), (102),(110),(103) and (112) were also present. Sample B have an intense peak at 34.86° corresponding to (100) plane and another peak of lesser intensity corresponding to (200) plane. Comparing the characteristic peaks intensities of samples A and B, the peak intensity of sample due to hybrid annealing is higher than normal annealing process. The peaks characteristic are higher in intensity and smaller in spectral range, suggesting strong crystalline activity on the films. No impurity peaks are identified, indicating that the end products comprise purely of ZnO **[Zhu Jian-yu *et al*., 2009].**

The ZnO films' crystallite size was determined by using Scherrer method **[Nanda Shakti *et al*., 2010].** Table 8 gives the crystallite size along prominent diffraction planes for films A and B. The size of the grains is found to be in samples from hybrid annealing is greater than from normal annealing process.

Table 8: Crystallite size along prominent diffraction planes for ZnO thin films.

Type of Annealing	(hkl)	2□ (degrees)	β (FWHM)	Particle size (nm)
Open air	(100)	31.8602	0.30900	27
Hybrid	(100)	31. 8642	0.23550	35

The sample's morphology is observed using FESEM pictures taken for samples A and B as depicted in Fig. 17. It is noted that the crystallites found in sample A is uniform and regular shape. The morphology of sample B is hazy and the crystallites are not clearly seen. Energy dispersion spectrum of sample gives the atomic contents of ZnO thin film corresponding to sample A and B (Fig.18)

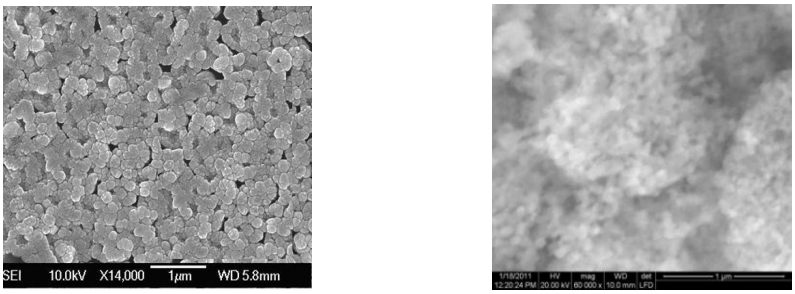

(a) (b)

Fig 17 SEM picture of ZnO layers grown on glass substrates `(a) sample A and b) sample B

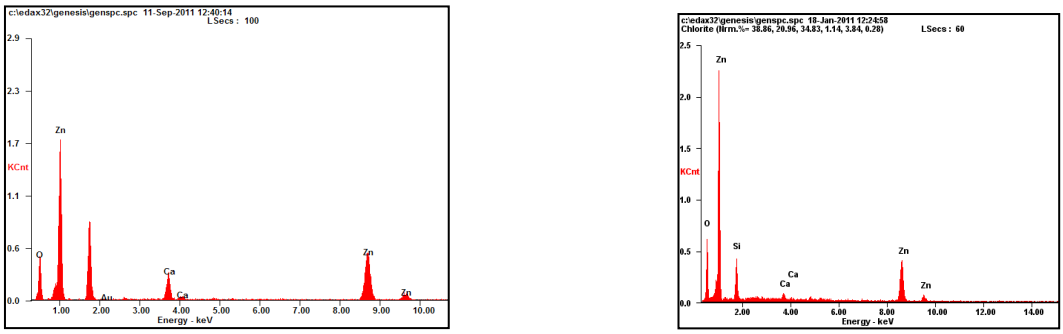

Fig.18 EDAX analysis for ZnO thin film (sample A and B)

2. OPTICAL PROPERTIES OF THIN FILMS

In order to study the optical properties of thin films, the absorbance was evaluated as a wavelength function in the range of 350-850 nm as given in Figure 19(a). The expression for absorption coefficient α is given by equation. The fundamental absorption, which relative to the transition from valence band to conduction band, can be used to find the optical band-gap (E_g) by the equation .

As ZnO is a direct transition material, the values of direct band-gap energy (E_g) obtained from the linear portion of the curve by extrapolation to zero of $(\alpha h\square)^2$ to the energy(E) intercept. Fig.19b shows the optical band-gap curve obtained from $(\alpha h\square)^2$ vs. (hu) for the transmittance spectra of samples A and B. Band-gap values are 3.13 and 3.34 eV for open air annealing and hybrid annealing respectively.

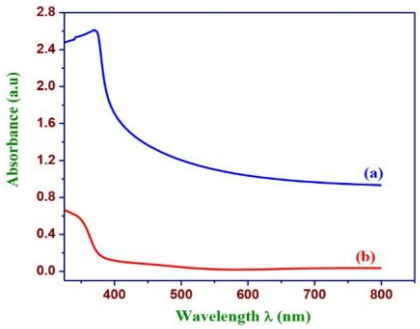

Fig 19(a) Absorption spectra of the spin coated thin film with different annealing processes

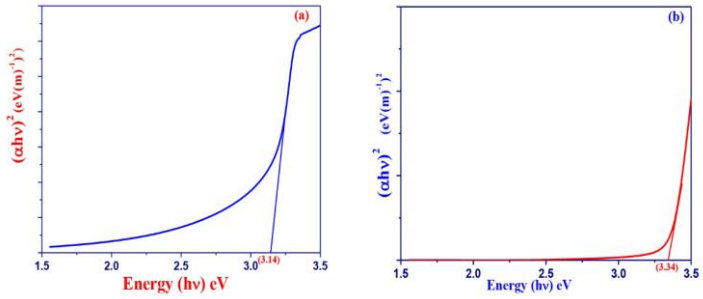

Figure 19(b) ($\alpha h\square$)^2 vs. (hu) plot based on the transmittance spectra

Fig..20 shows the photoluminiscence spectra of sample A (curve a) and B (curve b) taken at room temperature. Two peaks are seen for both the samples. A sharp UV band- edge emission centered at 383 nm and green bands centered at 525 nm are seen for sample A.

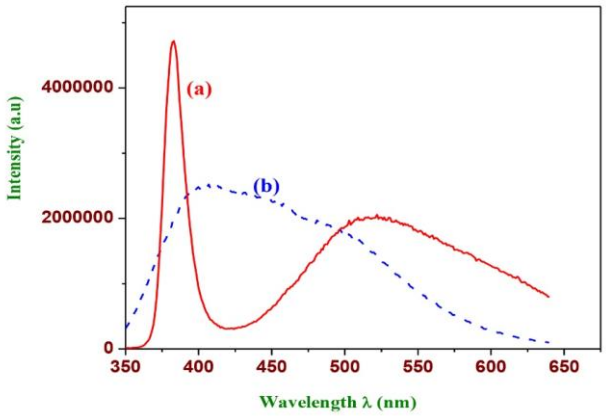

Fig 20 PL spectra of ZnO thin films annealed in open air and in hybrid annealing processes

The PL signal at 383 nm is a standard near-band edge ZnO (NBE) ultraviolet (UV) emission, suggesting a simple recombination of excitons into an exciton-exciton collision cycle **[Jianguo Lu et al., 2010, Yaoming Li et al., 2010**] and a deep-level green transition at 525 nm is typically dependent on the inclusion of the surface ionized oxygen vacancy. This recombination's results of a photo-generated hole with a single ionized charged state of the defect in ZnO [**Kenanakis *et al*., 2007, de Moura *et al*., 2010].** A broad blue band centred at 407 nm and shoulder peak at 489 nm are present for sample B. The NBE emission of sample A shifts towards red in comparison with sample B which might be ascribed to the size effect **[Wang *et al*., 2003]** which is supported from the different particle size of samples A and B calculated using XRD results.

VII CONCLUSION

Highly transparent ZnO thin films have been prepared successfully on glass substrate using the spin coating method. The effect of annealing was extensively investigated on the structural, photoluminescence and optical properties. XRD studies indicate that the crystallanity is enhanced on annealing and the average crystalline grain size also increases with annealing. The magnitude of the optical band gap as calculated from the optical result is consistent with the works observed. The ZnO thin films photoluminescence spectra shows a high excitonic UV value.

Consequently, it was seen that the effect of annealing makes a significant change on the structural and optical properties of ZnO spin coated thin films. A high optical quality of the deposited ZnO films would potentially allow their use of UV light emission. From the above results, it may be concluded that the ZnO thin films could be annealed at 450^{0}C is of good quality and it could be used for application purposes.

From the patterns of XRD of undoped ZnO thin films with different thickness, where all samples show similar diffraction peak positions. No peaks were detected as impurity levels, suggesting a high purity of the ZnO thin film acquired via the sol-gel technique. The experimental findings revealed that both the ultraviolet emissions in the PL spectrum and the magnetic properties are naturally determined by the film's thickness. The presence of sharp UV emission line as well as the LO-phonon lines indicates that these films have good crystalline quality. Higher thickness drastically changes the photoluminescence of spectra and shoulder peak disappears.

On the basis of the structural and optical studies conducted by adjusting the number of layers of ZnO film, it was discovered that eight-layer film exhibits high crystalline consistency with the prominent (002) peak which is the characteristic peak of the c-axis centered ZnO structure. The morphology of the eight-layer sample once again revealed hexagonal growths representing the simple cell structure of the unit.. Hence, further doped ZnO

RRIJM 2015, All Rights Reserved

films preparation was carried out with eight layer thickness annealed at 450°C in open air.

The effects of different kinds of annealing on the structural and optical properties were investigated. The XRD results show that the ZnO thin films annealed in open air is polycrystalline in nature having lesser crystallinity compared with the sample prepared using hybrid annealing. Photoluminescence studies show that the intensity of NBE emission in sample B is lesser than that of sample A. Enhancement of NBE emission is clearly observed in sample A which was annealed in open air environment. The increase in NBE emission intensity during open air annealing might be because of the presence of excess oxygen compared to the hybrid annealing process. Thus, there is a significant difference in the structural and optical properties of ZnO thin films which were undergone different types of annealing processes. Further work was continued with open air annealing.

References

1. Mingsong Wang, Sung Hong Hahn , Eui Jung Kim , Jae Seong Kim , Sunwook Kim, Chinho Park, Kee-Kahb Koo, Thin Solid Films, 516 (2008) 8599–8603.
2. Krasimira Shtereva, Vladimir Tvarozek, Pavel Sutta, Jaroslav Kovac and Ivan Novotny, Micro Electronic and Mechanical Systems, Kenichi Takahata, ISBN 978- 953-307-027-8, P. 572, December 2009, INTECH, Croatia.
3. Mondal.S, K. P. Kanta and P. Mitra, Journal of Physical Sciences, 12 (2008) 221- 229.
4. Bin-Zhong Dong and Guo-Jia Fang, Journal of applied physics, 101, 033713 (2007) 1-7.
5. Zhu Jian-yu , Zhang Jing-xia, Zhou Hui-fen,Qin Wen-qing, Chai Li-yuan, Hu Yue- hua, Trans.Nonferrous Met.Soc. China, 19 (2009) 1578-1582.
6. Nanda Shakti, Applied Physics Research, 2(1) (2010) 19-28.
7. Jianguo L u, KaiHuang, JianboZhu, XuemeiChen, XuepingSong, ZhaoqiSun, Physica B, 405 (2010) 3167–3171.
8. Yaoming Li, Linhua Xub, Xiangyin Li, Xingquan Shen, Ailing Wang, Applied Surface Science, 256 (2010) 4543–4547.
9. Kenanakis.G, M. Androulidaki, E. Koudoumas, C. Savvakis, N. Katsarakis, Superlattices and Microstructures, 42 (2007) 473–478
10. De Moura.A.P, R.C. Lima, M.L. Moreira, D.P. Volanti , J.W.M. Espinosa , M.O. Orlandi, P.S. Pizani, J.A. Varela, E. Longo, Solid State Ionics, 181 (2010) 775–780.

RRIJM 2015, All Rights Reserved